

# Thermal Modelling for Laser Treatment of Port Wine Stains

Li Dong<sup>1</sup>, Wang Guo-Xiang<sup>2</sup> and He Ya-Ling<sup>1</sup>

<sup>1</sup>State Key Laboratory of Multi-Phase Flow in Power Engineering  
Xi'an Jiaotong University; Xi'an,

<sup>2</sup>Department of Mechanical Engineering; The University of Akron; Akron,

<sup>1</sup>China

<sup>2</sup>USA

## 1. Introduction

Port Wine Stains (PWS) are congenital vascular birthmarks (see Fig. 1) that occur in approximately 0.3% of children (Alper & Holmes, 1983). Clinically, PWS ranges in appearance from pale pink to red to purple. Most of the lesions are pale pink at birth and can progressively be darken and thicken with age. PWS can be associated with significant cosmetic disfigurement and psychologic distress. Histopathological analysis of PWS reveals a normal epidermis overlying an abnormal plexus of benign vascular malformations consist of ectatic capillaries of diameters varying from 10 to 300  $\mu\text{m}$ . Laser treatment of PWS started in the late 1960s with continuous-wave lasers such as carbon-dioxide and argon lasers (Gemert et al., 1987; Dixon et al., 1984). During the laser treatment, light is absorbed by hemoglobin (Hb) and oxyhemoglobin (HbO<sub>2</sub>) (the principle chromophores for light absorption in human tissue) within the blood vessels and then converted into heat which damages the endothelium and surrounding vessel walls (Alora & Anderson, 2000). Unacceptable side effects such as scarring and permanent dyspigmentation were the two major shortcomings of the early laser treatment of PWS. Those side effects result from unselective heating of both PWS and nearby healthy dermal tissues during laser irradiation.



Fig. 1. PWS before and after laser treatment (Curtsey of Drs. Wang and Ying at Laser Cosmetic Centre of 2<sup>nd</sup> hospital of Xi'an Jiaotong University, Xi'an, China)

The principle of selective photothermolysis of Anderson and Parrish (Anderson & Parrish, 1983) revolutionized the laser treatment of vascular lesions such as PWS. Based on this principle, one can selectively destruct the PWS while keep the surrounding tissues untouched by properly choosing right laser wavelength and pulse duration. In the case of PWS, the primary absorption peaks of oxyhemoglobin and deoxyhemoglobin fall in the visible range (418, 542, or 577 nm) (see Fig. 2). For those wavelengths the water (another major chromophore for light absorption within tissue) has almost no absorption. Therefore, lasers with these wavelengths can effectively damage the PWS while does not cause any irreversible effect on surrounding tissues. As shown in Fig. 2, however, the melanin (another chromophore for light absorption) within epidermis also has strong absorption over the same wavelength range. Strong absorption of melanin and resulting epidermal heating not only lead to undesired skin injury but also reduce the heating effect of PWS which is buried deep underneath the epidermis. As a result, long wavelength lasers, such as the pulsed tunable dye lasers (PDL) with wavelengths of 595 – 600 nm, are now widely employed in laser treatment of PWS due to relatively weak absorption of melanin at the chosen wavelengths. In addition, the modern PDL lasers are often equipped with adjustable laser pulse width from 0.45 ms to 40 ms as well as surface cooling devices (Kelly et al., 2005).

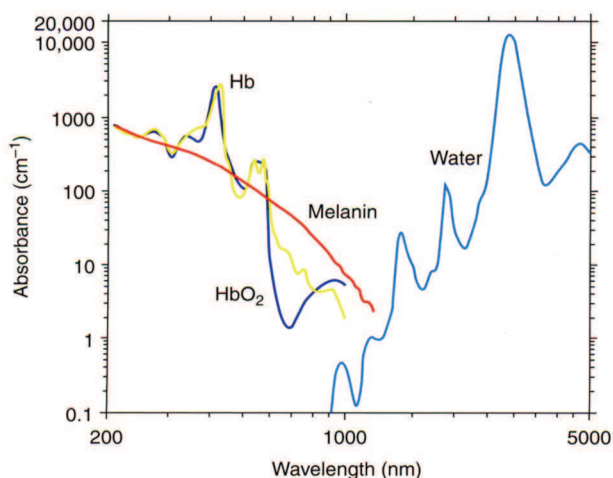


Fig. 2. Absorption spectra of major chromophores in skin (Anderson, 1997)

Surface cooling is critical in success of modern laser treatment of PWS (Kelly et al. 2005). The objective of surface cooling is to increase the laser fluence while prevent epidermal heating due to competitive absorption by epidermal melanin. Various cooling devices have been developed from early ice cubes (Gilchrest et al., 1982), chilled sapphire windows cooled by circulating refrigerant (Kelly et al., 2005), to present chilled air cooling (Hammes et al., 2005) and cryogen spray cooling (Nelson et al., 1995). The cryogen spray cooling technique provides spatially selective cooling of epidermis with pulse spray of volatile refrigerant R134a (tetrafluoroethane [C<sub>2</sub>H<sub>2</sub>F<sub>4</sub>]; boiling point at -26.2°C). Due to its short spurt, the PWS buried deep within dermis will be not affected. Consequently, PDL laser with cryogen spray cooling becomes standard protocol of PWS treatment (see Fig. 3).

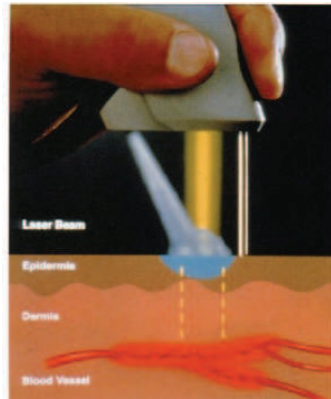


Fig. 3. Schematic of the laser treatment of PWS together with cryogen spray cooling (CSC). (Lanigan, 2000)

The laser surgery process of PWS (Laser PWS) has been studied extensively through mathematical modeling. Various models have been developed to better understand the laser-tissue interaction, in particular the thermal response of biological tissues and physiological mechanisms of thermal damage of PWS (see e.g., Pfefer et al., 2000; Pickering et al., 1989; Shafirstein et al., 2004; Tunnell et al., 2003). The models have also been used for optimization of the surgery parameters and for development of new treatment protocols (Jia et al., 2006, 2007). To model laser PWS, various simple skin models have been proposed to simplify the complex anatomic structure of the skin with PWS (Gemert et al., 1995). Mathematic techniques have been developed to calculate the light propagation and energy deposition within the PWS (Jacques & Wang, 1995). Energy absorbed by PWS can then be incorporated into the temperature equation as a heat source to determine the corresponding temperature change in the irradiated tissues. A thermal injury sub-model is also used to quantify the thermal damage to the PWS (Pearce & Thomsen, 1995).

The propagation of light in turbid media such as skin can be described by the radiative transport equation (Ishimaru, 1989) which cannot be solved analytically for tissue geometries. Techniques such as diffusion approximation (Gemert et al., 1997) and Beer's law (Verkruyssen et al., 1993) have been used in the literature but they are limited to highly scattering or coherent radiance materials (Niemz, 1996). For skin tissue, the Monte-Carlo (MC) method, which offers a flexible approach to track the photon transportation in a biological tissue, is widely accepted now as an accurate method and has been used in modeling of laser surgery (Keijzer et al., 1991; Lucassen et al., 1996; Pfefer et al., 1996; Smith & Butler 1995; Wang et al., 1995 & Wilson & Adam, 1983).

The bio-heat transfer equation such as Penn equation based on the skin models, in consistent with that used for light simulation, can be solved for tissue temperatures in laser PWS. Due to limited irradiation time of pulsed laser in laser PWS, the perfusion effect in Penn equation is usually neglected so that the bio-heat equation becomes a heat conduction equation. The thermal properties of PWS skin are scarce and those for normal skin tissues and blood are usually employed as an approximation. For laser PWS, cryogen spray cooling is widely employed by spraying volatile refrigerant such as R134a on skin surface before laser irradiation. Therefore, the cooling of skins before laser irradiation should be part of the model of laser PWS (Jia et al., 2006; Li et al., 2007a,b)

In this chapter, we will first present a brief review of the development of various skin models proposed in the literature for thermal modeling of laser PWS. Next, we explain the basic principle of the multi-layer Monte-Carlo method which is widely used for simulation of light propagation in the skin with PWS. Then we introduce a general relation developed recently by the present authors to quantify the heat transfer of cryogen spray cooling in laser PWS. Finally, results from a multi-layer, homogeneous model of laser surgery of PWS are presented to illustrate typical thermal characteristics of laser surgery of PWS. The effect of laser wavelength and laser pulse duration on the heating of the PWS layer is also examined briefly. Future needs for modeling the laser surgery of PWS is then discussed in conclusion.

## 2. Skin models and numerical simulation of laser surgery of PWS

The human skin has three main layers, the epidermis, the dermis, and the subcutaneous layer (fat) (Brannon, 2007). The epidermis is the outer layer of skin with its thickness varying in different types of skin. It is made up of cells called keratinocytes, which are stacked on top of each other, forming different sub-layers. In the stratum basale sub-layer, there are cells called melanocytes that produce melanin which is one of three major chromophores for light absorption. Melanin is a pigment that is absorbed into the dividing skin cells to help protect them against damage from sunlight (ultraviolet light). The amount of melanin in skin is determined by genes and by how much exposure to sunlight. Below the epidermis is the layer called dermis, which is a thick layer of fibrous and elastic tissue (made mostly of collagen, elastin, and fibrillin) that gives the skin its flexibility and strength. The dermis contains nerve endings, sweat glands and oil glands, hair follicles, and blood vessels. The blood vessels of the dermis provide nutrients to the skin and help regulate body temperature. Port Wine Stains (PWS) are the result of malformation of significant amount blood vessels within dermis. The subcutaneous tissue is a layer of fat and connective tissue that houses larger blood vessels and nerves. This layer is important in the regulation of temperature of the skin itself and the body. The size of this layer varies throughout the body and from person to person.

Ideally, a real three-dimensional multi-component skin models with detailed anatomic structure of PWS vessels should be used to evaluate the light distribution and temperature variation during laser PWS (Pfefer et al., 1996). However, low resolution of noninvasive imaging technique and extremely complex human tissue structure makes this impossible at moment. Thus, simplified skin models have been developed to analyze the thermal response of complex human skin with PWS under laser irradiation (Gemert et al., 1995). A simplified skin model should represent important histological characters of target chromophores and physical events during and after laser surgery and should be easily handled mathematically. The simplest model for laser PWS is probably the two-layer homogeneous model proposed first by Gemert and Hulsbergen (Gemert & Hulsbergen, 1981) who simplified the human skin containing PWS blood vessels to two-layer structure that parallel to the skin surface. In their model, the upper epidermis layer includes uniformly distributed melanin and the lower dermis layer is mixed with extra blood representing PWS. Gemert and Hulsbergen were the first who attempted to calculate the light distribution within PWS theoretically by employing the Kubelka-Munk method which significantly simplifies the light transport equation. Refined skin models as shown in Figure 4 with multi-layers (Gemert et al., 1982, 1995; Miller & Veith, 1993) have then subsequently been developed, all including an extra blood layer buried between dermis to represent the PWS. The Kubelka-Munk method and later the Monte-Carlo method were used to predict the light deposition within the PWS.

The multi-layer model with homogeneously distributed chromophore (blood) in the PWS layer has been widely used in numerical simulation of laser treatment of skin lesions. For example, Pickering and Gemert (Pickering & Gemert, 1991) used this model to theoretically investigate the mechanism of superior treatment of PWS by the laser of 585nm over that of 577nm. They found that the 585nm laser produced a deeper depth of vascular injury. The effects of various laser parameters such as pulsed duration, the repetition rate of pulses, the beam spot size, and the radiant energy fluencies on the outcomes of the laser surgery in PWS were systematically investigated (Gemert et al., 1995, 1997; Kienle & Hibst, 1995, 1997; Verkruysse et al., 1993). In all these studies, the PWS layer is treated as homogeneous mixture of dermal tissue and blood of a given volumetric fraction. The average optical and thermal properties of the chromophores and non-chromophore tissues weighted by their volumetric fractions are employed in the analysis. It is found that the calculated temperature in the PWS layer seems to be lower than expected (Aguilar et al., 2002), probably due to the use of the averaging properties in the calculations.

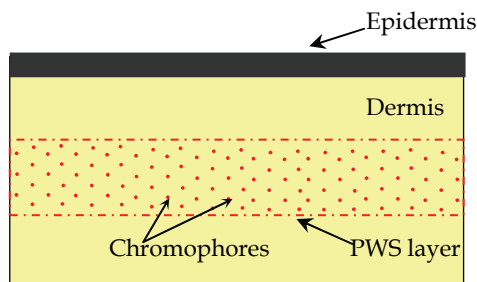


Fig. 4. Schematic of a multi-layer skin model including a PWS layer within dermis. The PWS layer is made of normal dermal tissue mixed homogeneously with blood

The multi-layer skin model simply treats the PWS as a homogeneous mixture of dermal tissue and blood, ignore the detailed structural characteristics of blood vessels in PWS. To represent more realistic anatomic features of PWS, skin models that contain individual blood vessels have been developed (Gemert et al., 1986; Lahaye & Gemert, 1985; Lucassen et al., 1995; Pickering et al., 1989), as shown in Figure 5. For example, Anderson and Parrish (Anderson & Parrish, 1983) performed a thermal analysis directly on an isolated blood vessel that was buried in dermal tissue and under laser irradiation. This analysis led to their famous “selective photothermolysis” theory that provides theoretical foundation for laser design and selection and for development of clinic protocol of laser treatment of PWS and other cutaneous diseases (Lanigan, 2000). With the rapid growth of the computing power, skin models with discretely distributed individual blood vessels became the favored among researchers. Skin models with the blood vessels that are parallel to the skin surface and regularly (aligned or staggered) buried in the dermis underneath the epidermal layer have been widely employed. Recently, models with randomly distributed blood vessels with varying sizes have also been utilized. Occasionally, the model with a single blood vessel was also used to test the clinic outcome of new treating protocols of laser PWS (Jia et al., 2006, 2007). Concerns have been raised for possible lack of the scattering and shielding effects of numerous blood vessels in real PWS for those discrete blood vessel models (Tan et al., 1990; Verkruysse et al., 1993).

The skin model with discrete blood vessels can provide direct visualization of heating of the blood vessels in laser PWS (Baumler et al., 2005; Shafirstein et al., 2004, 2007; Tunnell et al., 2003). For example, Smith and Butler (Smith & Butler, 1995) have shown that the blood vessels are heated up first during laser irradiation, and the dermis surrounding the vessel are then heated conductively by the high temperature vessels. The effect of local heating within the vessel and the shadowing effects of front vessels over the bottom vessels have also been demonstrated.

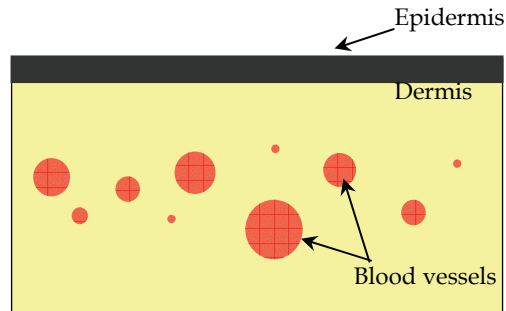


Fig. 5. Schematic of a skin model with discrete blood vessels buried in dermis

### 3. Multi-layer Monte-Carlo (MC) method for light propagation in skin tissue

All above skin models can be treated as a multi-layered structure, even for those with discretely distributed blood vessels (see Figs. 4 & 5). The light propagation within such multi-layered structure can be accurately simulated by the multi-layered Monte-Carlo (MLMC) method developed by Wang et al., (Wang et al., 1995). Here a brief introduction of the MLMC method is presented and the details can be found elsewhere (Jacques & Wang, 1995; Wang et al., 1995).

The MLMC method deals with the transport of a laser beam within a medium made of layered tissues that are parallel to each other. In MLMC, a photon packet is first injected perpendicular to the tissue surface with a unit weight ( $W = 1$ ) with the position of the photon packet on the surface (position O in Figure 6) is determined from the shape of the beam profile (e.g., Gaussian). The propagation or movement of the photon packet in the tissue is then tracked step by step. At each step, the step size between two collisions within the tissue is determined from a logarithmic distribution function with a random number generated by the computer. Since the photon packet may hit a boundary of the current layer, before each photon movement, the distance between the current photon location and the boundary of the current layer in the direction of the photon propagation needs to be computed. If the step size is smaller than the calculated distance, the step will move within the current layer (segment OA, see Figure 6). Otherwise, if the step size is greater than this distance (segment AB), the photon packet will hit the boundary and the photon packet can be either internally reflected or transmitted across the boundary. If the photon is internally reflected, the photon packet continues propagation with an updated step size and changes its direction as a mirror reflection (segment BC). If the photon is transmitted, it continues its propagation with an updated step size but with the direction newly calculated according to

the Snell's law (segment BD). At the end of each step, the photon packet will interact with the tissue. A fraction of the photon weight ( $\Delta W = \mu_a / \mu_t$ ) is first absorbed at the interaction site, where  $\mu_a$  and  $\mu_t$  are the absorption coefficient and the attenuation coefficient, respectively, of the medium. The absorbed weight is scored into the absorption array  $A[i,j]$  at the local volume element  $(i,j)$  in a two-dimensional grid system, where  $i$  and  $j$  are the indices for volume elements. After absorption, the photon packet updates its weight to  $W - \Delta W$  and is then scattered at the interaction site (segment DE) by choosing a new direction of propagation according to a given phase function and another random number generated by the computer.

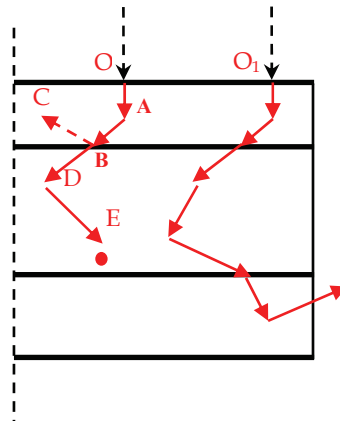


Fig. 6. A schematic showing movement of photon packets in multi-layer Monte Carlo simulation

The weight of a launched photon packet is continuously decreased due to absorption by the medium as the photon packet moves within the tissue step by step. The photon packet is terminated naturally if it moves out of the tissue domain due to either reflection or transmission. For a photon packet still propagating inside the medium, the Russian roulette technique is used to terminate the photon packet when the photon weight  $W$  is reduced to be lower than a given threshold value. Once the photon packet is terminated, a new photon packet enters the skin domain, probably at a new position (for example  $O_1$  in Figure 6), and the above process is then repeated.

After all photon packets terminate, the MLMC simulation completes and the final absorption array  $A[i,j]$  is obtained for the entire domain. Then, the energy density deposited in each grid element can be calculated as follows:

$$Q[i, j] = E \cdot \pi r^2 \cdot \frac{A[i, j]}{N \cdot dv} \quad (1)$$

where the array  $Q[i, j]$  is the rate of energy storage in the volume element  $(i,j)$ ,  $E$  is the incident energy of the laser,  $r$  is the spot radius of the incident laser,  $N$  is the total number of photo packets used in the simulation, and  $dv$  is the volume of the element. Although the light transport in the layered-skin structure is gridless, the selection of the size of the volume element in the grid affects the simulation through Equation (1). The size of the volume

element should be selected appropriately for proper scoring of the absorbed energy within the element by satisfying the statistical requirement of the MC simulation. There should have enough photons that have arrived at any given element in order to rightly reflect the photon absorption in the medium. If the size of the volume element becomes too small and the total number of photons used in the simulation is limited, one may find the case that no photons at all arrive at certain elements and no energy deposition is registered in those elements. Recently, the present authors have developed criteria that can be used to choose right element size and the total number of photon packets needed in the MC simulation (Li et al., 2011).

#### 4. Cryogen spray cooling (CSC)

During the laser treatment of PWS, a significant amount of laser energy is absorbed by melanin within the basal layer of the epidermis (Tunnell et al., 2000). To allow higher laser energy doses used in clinic, one needs to cool the epidermis prior to laser irradiation. Cryogen spray cooling (CSC) is one of the techniques developed to protect the epidermis from non-specific heating by pre-cooling the skin prior to laser irradiation (Nelson et al., 1995). The cryogen utilized is 1,1,1,2 tetrafluoroethane, also known as R134a, with boiling temperature of  $T_b = -26.2$  °C at atmospheric pressure. Cryogen is usually kept in a container at saturation pressure, which is approximately 660 kPa at 25 °C (95.7 psi), and delivered through a standard high pressure hose to an electronically controlled fuel injector, to which a straight-tube nozzle is attached. As the cryogen reaches the tissue surface, tissue experiences a quick cooling process to reach low temperatures (Kelly et al., 2005).

To model laser PWS with CSC, a convective thermal boundary condition is usually used (Aguilar et al., 2002; Jia et al., 2007; Li et al., 2007a,b; Majaron et al., 2001; Pfefer et al., 2000). Due to lack of experimental data, the early models of laser PWS have employed a constant heat transfer coefficient to quantify the short-pulsed cooling process (Aguilar et al., 2002; Majaron et al., 2001; Pfefer et al., 2000). Recently, extensive experimental and numerical investigations have been conducted to characterize the cryogen spray (Pikkula et al., 2001; Zhou et al., 2008a,b) and to quantify the convection heat transfer during spray (Aguilar et al., 2003a,b; Franco et al., 2004, 2005; Jia et al., 2004, 2007). Based on these experimental data, the present authors have developed a quantitative relation that can be used to estimate the convection heat transfer coefficient,  $h(r,t)$ , as a function of both the space ( $r$  on the skin surface) and time ( $t$ ) during CSC in laser PWS (Li et al., 2007a,b). The non-dimensional form of the relation is given as follows:

$$\left\{ \begin{array}{ll} h^*(r^*, \tau) = \begin{cases} h_o^*(\tau) & 0 \leq r^* \leq 0.4 \\ [5(1-r^*)] / [3h_o^*(\tau)] & 0.4 < r^* \leq 1.0 \end{cases} & \tau \leq 1.0 \\ h^*(r^*, \tau) = \begin{cases} h_o^*(\tau) & 0 \leq r^* \leq 0.2(\tau+1) \\ h_o^*(\tau) + \frac{(5r^* - \tau - 1)}{(4-\tau)} \times [0.09(\tau-1) - h_o^*(\tau)] & 0.2(\tau+1) < r^* \leq 1.0 \end{cases} & 1.0 < \tau < 4 \\ h^*(r^*, \tau) = h_o^*(\tau) & 0 \leq r^* \leq 1.0 \quad \tau \geq 4.0 \end{array} \right. \quad (2)$$

with  $h_o^*(\tau)$  as the non-dimensional heat transfer coefficient at the center of spray:

$$h_o^*(\tau) = \frac{h_o(t)}{h_{o,max}} = \begin{cases} \tau & \tau \leq 1.0 \\ 1.0 - 0.35(\tau - 1) & 1.0 < \tau \leq 3.0 \\ 0.3 - 0.02(\tau - 3) & 3.0 < \tau \leq 8.0 \\ 0.2 - 0.0125(\tau - 8) & 8.0 < \tau \end{cases} \quad (3)$$

where  $h_o(t)$  is the dimensional heat transfer coefficient at the center of spray and  $h_{o,max}$  is the maximum value of  $h_o$  at time  $t_{max}$ , both estimated from experimental data (Li et al., 2007a). In Eqs. (2) and (3), the non-dimensional heat transfer coefficient,  $h^*$ , the non-dimensional radius coordinate,  $r^*$ , and the non-dimensional time,  $\tau$ , are defined as follows:

$$h^*(r^*, \tau) = h(r, t) / h_{o,max}, \quad r^* = r / r_{spray}, \quad \text{and} \quad \tau = t / t_{max}$$

with  $r_{spray}$  the radius of spray spot on the skin surface.

Equations (2) and (3) can be employed in any thermal models for laser PWS before laser irradiation. Figure 7 shows typical dynamic variations of the temperature in the skin during CSC calculated by our own model (to be discussed in detail below). In Figure 7, the temperature distributions within the skin are plotted at two time instants during spray. The corresponding spray distance is 30mm and the spray spurt is 100 ms. One point to be noticed is that the skin surface temperature drops to about -20 °C at 30 ms after the spray starts (see Figure 7a). At this time, however, the temperature within the skin including majority of the epidermal layer still remains the same initial value. After 60 ms of CSC (Fig. 7b), the entire epidermal layer is cooled down below -10 °C, but the temperature of the PWS layer still remains almost the same initial temperature and is not affected by the spray. Such an effect of the cryogen spray is desirable for laser PWS since the only purpose of cooling is to prevent the skin overheating. Since the skin tissue is a very poor thermal conductor, the cooling effect at the surface is hardly felt by the PWS buried deep in the dermis if the spray spurt is kept short.

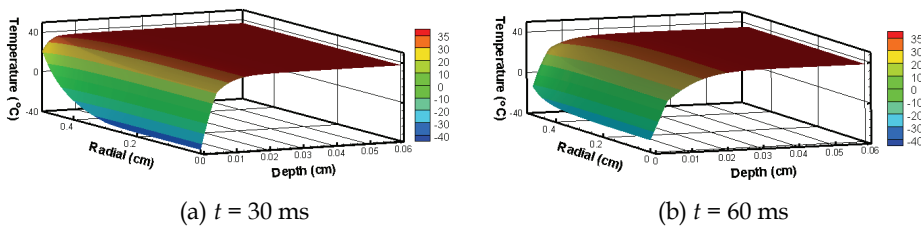


Fig. 7. Calculated temperature distributions within skin during cryogen spray cooling at times after 30ms (a) and 60ms (b). (Spray distance: 30 mm)

### 5. A model for laser treatment of PWS with CSC

To illustrate the thermal characteristics of the laser surgery process of PWS, we present here a multi-layer thermal model of laser PWS with CSC. The skin model chosen consists of four layers: an epidermal layer containing melanin, two dermal layers with a PWS layer sandwiched in between. The PWS layer is assumed to be a homogeneous mixture of dermis and blood of a given volumetric fraction. The bulk optical and thermal properties of the epidermal layer and the PWS layer are determined based on the corresponding volume

contents of melanin and hemoglobin (Verkruysse et al., 1993), respectively. The laser beam has a Gauss profile and the MLMC method discussed in Section 3 is used to quantify the energy deposition in various layers. The resulting rate of energy deposition in the tissue, given in Eq. (1), is included as the source term,  $Q_i$ , in the following heat conduction equation:

$$\rho_i c_{p,i} \frac{\partial T}{\partial t} = \frac{k_i}{r} \frac{\partial}{\partial r} \left( r \frac{\partial T}{\partial r} \right) + k_i \frac{\partial^2 T}{\partial z^2} + Q_i \tag{4}$$

where the subscript  $i$  ( $= e, d, p$ ) represents, respectively, the epidermal layer, the dermal layer, and the PWS layer;  $\rho$  is the density,  $c_p$  the specific heat,  $k$  the thermal conductivity,  $T$  the temperature, and  $t$  the time. A cylindrical coordinate system as shown in Figure 8 is used with the origin located at the center of the laser beam on the skin surface.

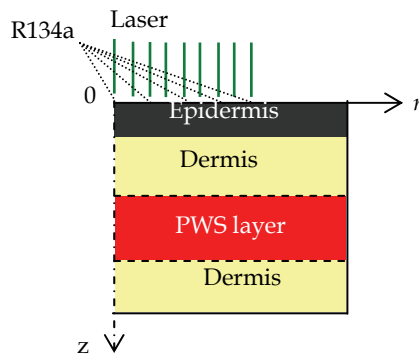


Fig. 8. Schematic of the multi-layer skin model and the corresponding two-dimensional cylindrical coordinate system

On the skin surface ( $z=0$ ), a convection heat transfer condition is used to describe the cooling effect of CSC and the heating effect of the environment afterward:

$$\begin{aligned} k_e \left. \frac{\partial T}{\partial z} \right|_{z=0} &= h_c(r,t)[T(r,0,t) - T_c] && \text{during CSC} \\ k_e \left. \frac{\partial T}{\partial z} \right|_{z=0} &= h_a[T(r,0,t) - T_a] && \text{after CSC or without CSC} \end{aligned} \tag{5}$$

where  $T_c$  and  $T_a$  are the temperatures of liquid cryogen on the skin surface and the environment, respectively.  $h_a$  is the convective heat transfer coefficient between the cold surface and air, and is treated as a constant.  $h_c(r, t)$  is the heat transfer coefficient between the surface and the liquid cryogen on the surface during short-pulsed cryogen spray and is determined from Eqs. (2) and (3).

The above model is used to simulate the thermal process in the laser treatment of PWS with CSC. The laser spot diameter is chosen as 5 mm while the CSC spray spot size is fixed at 10 mm. For the skin model, the thickness of the epidermal layer is 50  $\mu\text{m}$  with melanin of five volumetric percent (5%); the thickness of the PWS layer is 200  $\mu\text{m}$  with the volumetric fraction of hemoglobin of 30%. Here a high volumetric fraction of hemoglobin is used to

simulate the mature PWS lesion (dark red or purple). The initial skin temperature is assumed to be at 37 °C and the surrounding temperature  $T_a$  is 25 °C. Two typical wavelengths (585 nm and 595 nm) of the pulsed-dye lasers are examined with laser pulse duration varying from 1.5 ms to 40 ms, corresponding to the working range of the clinically-used PDL lasers (Kelly et al., 2005).

### 5.1 Light and temperature distribution without CSC

A typical result from the multi-layer Monte-Carlo simulation is given in Figure 9a which shows the distribution of the photon weight  $A(r, z)$  within the skin after irradiation of a PDL beam of 585 nm. As expected, a strong absorption occurs within both the epidermal layer ( $0 < z < 50 \mu\text{m}$ ) and the PWS layer ( $250 < z < 450 \mu\text{m}$ ) due to the existence of melanin and hemoglobin within the two layers, respectively. Less absorption in the PWS layer than that in the epidermal layer is due to the screening effect of the epidermal layer. It is such absorption by the melanin in the epidermal layer that prohibits the application of a high energy dose in laser PWS. Comparing to these two layers, the dermal layer shows very little absorption of light because of a low absorption coefficient of dermis at the given wavelength (585 nm). Figure 9a also shows a decrease of the photon absorption along the radial direction, due to the nature of the incoming laser beam which has a Gaussian profile.

The photon absorption given in Figure 9a can be converted into the rate of heat generation within the skin in the energy equation (4). Solving the energy equation gives the temperature distribution within the skin, as shown in Figure 9b. Figure 9b plots the temperature distribution within the skin at the end of 1.5 ms laser pulse. In this case, no cryogen spray cooling is used. The incident laser fluence was 4 J/cm<sup>2</sup>. It is found that both the epidermal and the PWS layers experience high temperatures due to strong photon absorption of the two layers. At the present level of laser fluence, the temperatures of both the epidermal and PWS layers exceed the critical coagulation temperature of about 70 °C (Pearce & Thomsen, 1995). Although a high PWS temperature is desired, a high epidermal temperature causes unspecified skin injury and should be avoided. The cryogen spray cooling technique can be used to protect the skin from such overheating as will be shown below.

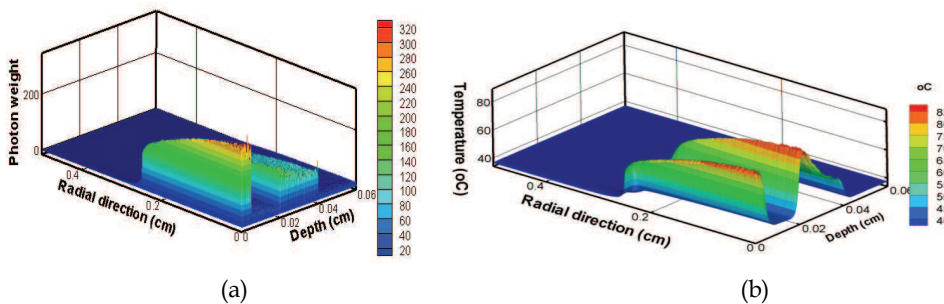


Fig. 9. Calculated distributions of the photon absorption (a) and temperature (b) within the skin at the end of 1.5 ms laser pulse of 585 nm. (Laser fluence  $E = 4 \text{ J/cm}^2$ , without CSC)

### 5.2 Thermal characteristics of laser treatment of PWS with CSC

The thermal characteristics of laser PWS with CSC are illustrated in Figure 10 which presents the temperature distributions within the skin at four time instants: 100ms (a),

101.5ms (b), 121.5ms (c) and 301.5ms (d) after the CSC starts. Laser was fired after 100 ms spurt cryogen spray. The laser fluence is 6 J/cm<sup>2</sup> and the laser pulse duration is 1.5ms. At the end of the CSC (Fig. 10a), the skin surface temperature decreases to below -10 °C while the temperature of the PWS layer remains almost the same as the initial value. At the end of laser irradiation (Fig. 10b at 101.5 ms), the temperatures of both the epidermal and the PWS layers rise as a result of energy absorption, while the temperature of the dermal layer keeps almost unchanged due to a low absorption of the dermis. After laser irradiation, the temperatures in both the epidermal and the PWS layers decrease as a result of heat conduction. As we can see from Fig. 10c (20 ms after laser irradiation), the peak temperatures of both the epidermal and the PWS layers lower down while the temperature of the dermal layer rises. As heat conduction continues, the entire skin layers approach almost uniform temperature, see Fig. 10d at 200 ms after laser irradiation.

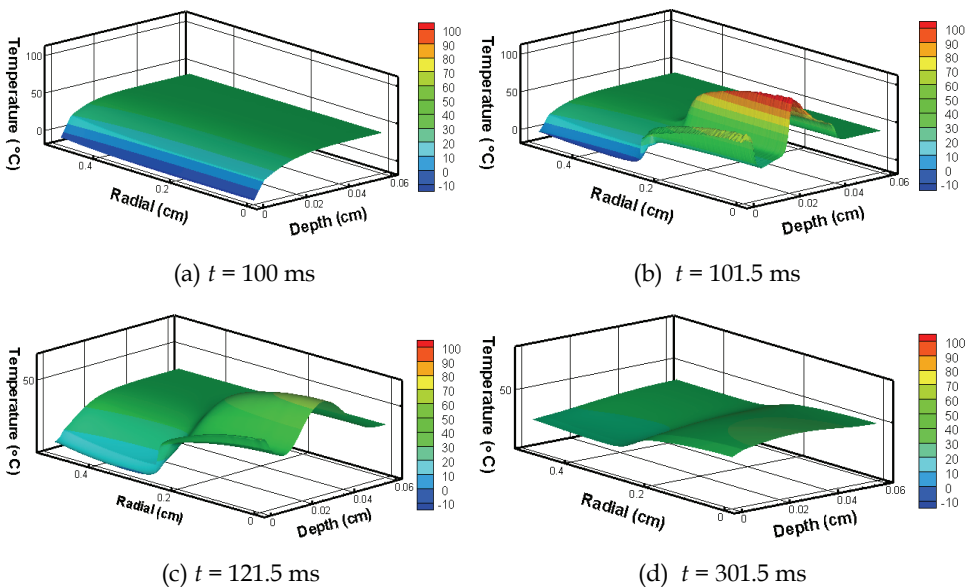


Fig. 10. Calculated temperature distributions within the skin during laser surgery of PWS with CSC at times after 100ms (a), 101.5ms (b), 121.5ms (c) and 301.5ms. (CSC spurt duration: 100ms, Spray distance: 30 mm, laser fluence: 6 J/cm<sup>2</sup>, and laser pulse duration: 1.5ms)

### 5.3 Effect of laser wavelength

Appropriate selection of the wavelength of the laser beam is a critical issue in laser PWS due to the sensitivity of the light absorption of PWS to the wavelength. Figure 11 shows the temperature distributions of the skin at the end of 1.5 ms pulsed laser irradiation under two wavelengths, 585 (a) and 595nm (b), respectively, with all other conditions remain the same. A comparison of the temperature profiles along the central axial direction corresponding to Figure 11 is also given in Fig. 12a. Figure 12b plots similar temperature distributions for a thicker PWS layer of 300  $\mu$ m. Inspecting these figures, one finds that the laser wavelength

affects the highest temperature possible in the PWS layer and the evenness of the temperature distribution over the PWS layer. A much higher possible temperature in PWS is achieved for the shorter 585 nm laser than that for the longer 595 nm laser. The longer 595 nm laser, however, produces a much more even heating over the PWS layer. This can be more clearly demonstrated in the case of a thicker PWS layer as shown in Figure 12b.

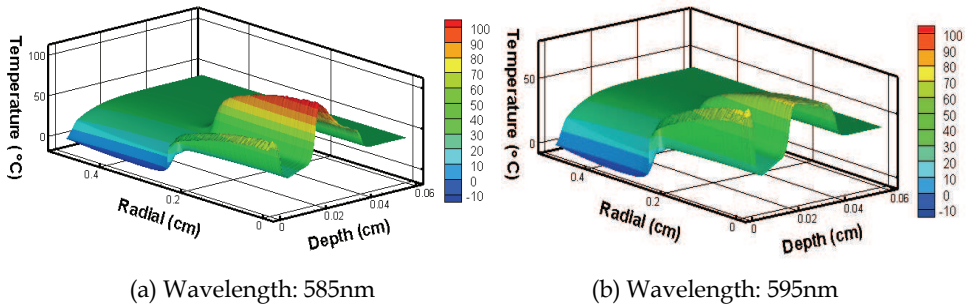


Fig. 11. Temperature distributions within the skin at the end of 1.5 ms laser irradiation. (PWS layer thickness: 200  $\mu\text{m}$ , laser fluence: 6 J/cm<sup>2</sup>, with CSC)

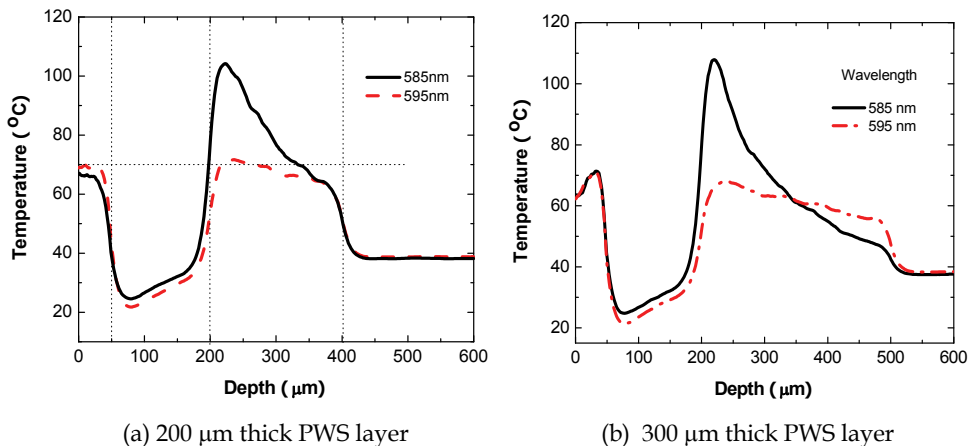


Fig. 12. Temperature distribution along the tissue depth direction at the spray center for two wavelengths (585 and 595nm): PWS layer thickness (a) 200  $\mu\text{m}$  and (b) 300  $\mu\text{m}$ . (Laser fluence: 6 J/cm<sup>2</sup>, pulse duration: 1.5 ms, with CSC)

**5.4 Effect of laser pulse duration**

The pulse duration of the laser beam is another important parameter that needs to be carefully chosen in clinic practice. Figure 13 shows the calculated temperature distributions within the skin at the end of laser irradiation for three pulse durations: 1.5 ms (a), 10 ms (b) and 40ms (c), respectively. The laser fluence is 6 J/cm<sup>2</sup>. The comparison of the central temperature profile within skin for three cases is given correspondingly in Figure 13d.

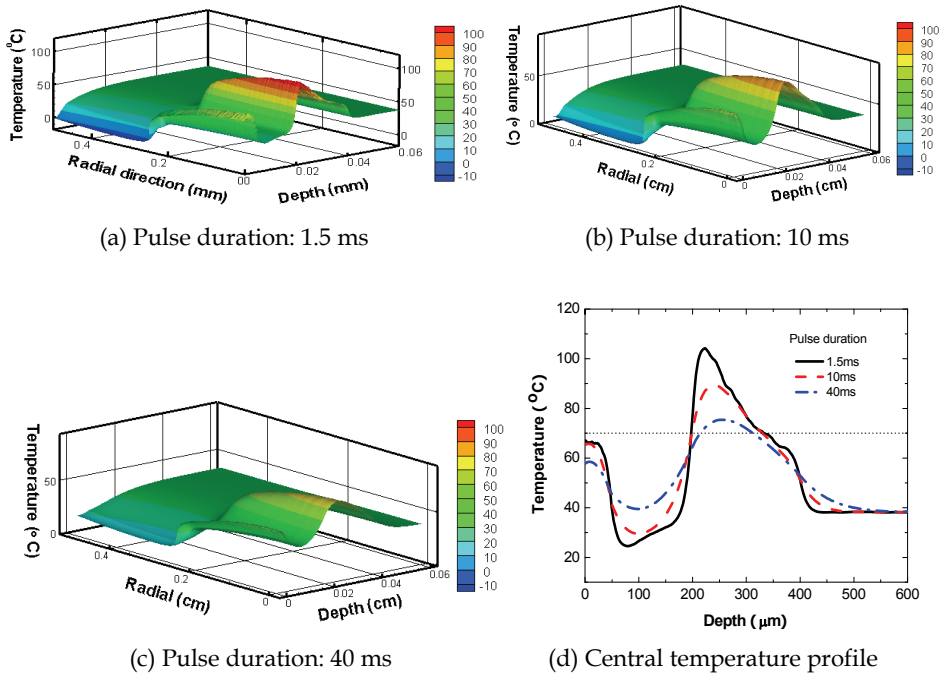


Fig. 13. Calculated temperature distributions within the skin at the end of laser irradiation for three pulse durations: (a) 1.5 ms, (b) 10 ms and (c) 40 ms; (d) Comparison of the central temperature profiles for three pulse durations. (Laser fluence: 6 J/cm<sup>2</sup> with CSC)

Inspecting these plots finds immediately that the peak temperature of the PWS layer at the end of laser irradiation shows a continuous reduction, from 105 °C to 73 °C as the pulse duration increases from 1.5 ms to 40 ms. In the case of a short pulse duration (e.g., 1.5 ms), the PWS layer is heated up quickly at the end of laser irradiation with little heating of the neighbor dermal tissue. A significant portion of the PWS layer is heated up over the critical coagulation temperature of 70 °C. When the pulse duration increases to 40 ms, not only the peak temperature of the PWS layer reduces to a lower value, the percentage of the PWS layer that is above the critical coagulation temperature is also significantly reduced to a smaller portion. Meanwhile, the neighbor dermal tissue is significantly heated up to close to the coagulation temperature, which may lead to the damage of the healthy tissues. Such a variation in the peak temperature of the PWS with pulse duration can be understood by considering the combined effect of the laser heating and heat conduction of the heated PWS to the neighbor colder dermis. As the laser heating prolongs over a long pulse, the heat conduction from the heated PWS layer to the surrounding colder dermal tissues prevents a further increase in the PWS temperature and thus reduces the peak PWS temperature. A longer laser heating time is also associated with more energy through conduction into the surrounding tissues, leading to continuous increase in the temperature of the dermal tissues. In clinic practice of laser PWS, a short laser pulse is usually preferred, except for the cases with extremely large blood vessels. For that case, however, a better model is needed to provide more quantitative description of the laser surgery process of PWS.

## 6. Conclusion and future work

In this chapter, we present a brief review of thermal modelling of the treatment of port wine stains with the pulsed dye laser. We show that laser treatment of port wine stains is primarily a thermal issue involving both radiative energy transport within the tissue during laser irradiation and tissue heat conduction during and after laser irradiation. Based on simplified skin models that reduce the complex anatomic structure of skins to simple layer structures, the process can be successfully simulated by solving the corresponding radiative energy transport with the multi-layer Monte-Carlo method and the heat conduction equation with traditional numerical methods. We have used a simple multi-layer homogeneous model to illustrate the basic thermal characteristics of laser treatment of PWS. We also demonstrated that the model can be used to make selections of the laser parameters such as wavelength and pulse width in clinical practice. Quantitative information for critical surface cooling technique, CSC, is also presented and included in our model.

Although great progresses have been achieved in both clinic practice and physical understanding of laser PWS after four decades' efforts, many issues remain. Clinically, the present protocol of PDL-based lasers could significantly eliminate the PWS vessels, but only less than 20% of complete clearance of the PWS has been achieved (Kelly et al., 2005). Recurrence has been observed with a rate up to 50% after five years (Orten et al., 1996). All these suggest a lack of fundamental understanding of the PWS destruction mechanisms in the present laser PWS process. From the modeling point of view, neither the multi-layer homogeneous model nor the discrete blood vessel model provides accurate representation of the real and complex anatomic configuration of the PWS vessels. Attempts to construct realistic PWS structure based on computer-reconstructed biopsy from PWS patients had only limited success (Pfefer et al., 1996). New models are desired that should combine the simplicity of the multi-layer homogeneous model while take into account the detailed effect of complex PWS configurations. In addition, quantitative predictions of the temperature change of the PWS in the laser treatment require accurate optical and thermal properties of PWS, which are scarce at the moment.

The ultimate objective of any model for laser PWS is to accurately predict the thermal damage after the laser irradiation. The existing PWS damage model is a pure thermal model based on simple Arrhenius rate process integral (Pearce & Thomsen, 1995). The model does not take into account the photochemical and photomechanical effect of laser on skin tissues and blood vessels. Recent experimental evidence suggests that the vessel damage in laser PWS is a multi-time scale phenomenon. The collateral damage of blood vessels in laser PWS is due to accumulative result of early photothermal effect and later photochemical and photomechanical effect. The recurrence of PWS involves a time scale that may last to more than five years. Active researches are being conducted to understand these long term phenomena in laser PWS.

## 7. Acknowledgments

We like to acknowledge valuable discussions with Drs. Y.X. Wang and Z.Y. Ying at Laser Cosmetic Centre of 2<sup>nd</sup> Hospital of Xi'an Jiaotong University. Special thanks to Prof. Guo Lie-jin, Prof. Chen Bin, Prof. Wang Yue-she, Dr. Zhou Zhi-fu and Dr. Wu Wen-juan for their help to the project. G.-X. Wang thanks the support of "Changjiang Scholar" program of Education Ministry of China. The work is supported in part by the special fund from the State Key Laboratory of Multiphase Flow in Power Engineering at Xi'an Jiaotong University.

## 8. References

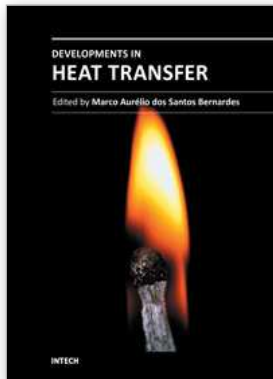
- Aguilar, G.; Diaz, S.H.; Lavernia, E.J. & Nelson, J.S. (2002). Cryogen spray cooling efficiency: improvement of port wine stain laser therapy through multiple-intermittent cryogen spurts and laser pulses. *Lasers in Surgery and Medicine*, Vol.31, No.4, (July 2002), pp. 27-35, ISSN 0196-8092
- Aguilar, G.; Wang, G.-X. & Nelson, J.S. (2003a). Effect of spurt duration on the heat transfer dynamics during cryogen spray cooling. *Phys Med Biol*, Vol.48, No.14, (July 2003), pp. 2169-2181, ISSN 0031-9155
- Aguilar, G.; Wang, G.-X. & Nelson, J.S. (2003b). Dynamic Cooling Behavior during Cryogen Spray Cooling: Effects of Spurt Duration and Spray Distance. *Lasers in Surgery and Medicine*, Vol. 32, No.2, (February 2003), pp. 152-159, ISSN 0196-8092
- Anderson, R.R. (1997). Laser-tissue interaction in dermatology, In: *Lasers in cutaneous and aesthetic surgery*, K.A. Arndt (Ed.), pp. (26-51), Lippincott Williams and Wilkins, ISBN 0316051772, Boston, Massachusetts, USA
- Anderson, R.R. & Parrish, J.A. (1983). Selective photothermolysis: precise microsurgery by selective absorption of pulsed radiation. *Science*, Vol.220, No.4596, (April 1983), pp. 524-527, ISSN 0036-8075 (Print), 1095-9203 (Online)
- Alora, M. B. T. & Anderson, R. R. (2000). Recent developments in cutaneous lasers. *Lasers in Surgery and Medicine*. Vol.26, No.2, (April 2000), pp. 108-118, ISSN 0196-8092
- Alper, J.C. & Holmes, L.B. (1983). The incidence and significance of birthmarks in a cohort of 4641 newborns. *Pediatr Dermatol.*, Vol. 1, No.1, (July 1983), pp. 58-68, ISSN 1525-1470 (Online)
- Baumler, W.; Vogl, A.; Landthaler, M.; Waner, M. & Shafirstein, G. (2005). Port wine stain laser therapy and the computer-assisted modeling of vessel coagulation using the finite elements method. *Medical Laser Application*, Vol.20, No.4, (December 2005), pp. 247-254, ISSN 1615-1615
- Brannon, H. (April 2007). Skin Anatomy, In: *About.com*, 10.04.2011, Available from: <http://dermatology.about.com/cs/skinanatomy/a/anatomy.htm>
- Dixon, J.A.; Huether, S.; & Rotering, R. (1984). Hypertrophic scarring in argon laser treatment of port wine stains. *Plast Reconstruct Surg*, Vol.73, No.5, (May 1984), pp. 771-780, ISSN 0032-1052 (Print), 1529-4242 (Online)
- Franco W.; Wang, G.-X.; Nelson, J.S. & Aguilar, G. (2004). Radial Heat Transfer Dynamics during Cryogen Spray Cooling. *Proceedings of IMECE 2004*, IMECE2004-59609, ASME, ISBN 0-7918-4711-X
- Franco, W.; Liu, J.; Wang, G.-X.; Nelson, J.S. & Aguilar, G. (2005). Radial and temporal variations in surface heat transfer during cryogen spray cooling. *Phys Med Biol*, Vol.50, No.2, (January 2005), pp. 387-397, ISSN 0031-9155
- Gemert, M.J.C. van & Hulsbergen, J.P.H. (1981). A model approach to laser coagulation of dermal vascular lesions. *Arch Dermatol Res*, Vol.270, No.4, (February 1981), pp. 429-439, ISSN: 0340-3696 (Printed) 1432-069X (Online)
- Gemert, M.J.C. van; de Kleijn, W.J.A. & Hulsbergen J.P.H. (1982). Temperature behaviour of a model port wine stain during argon laser coagulation. *Phys Med Biol*, Vol.27, No.9, (September 1982), pp. 1089-1104, ISSN 0031-9155

- Gemert, M.J.C. van; Welch, A.J.; & Amin, A.P. (1986). Is there an optimal laser treatment for port wine stains? *Lasers in Surgery and Medicine*, Vol.6, No.1, (January 1986), pp. 76-83, ISSN 0196-8092
- Gemert, M.J.C. van; Welch, A.J.; Tan, O.T.; & Parrish, J.A. (1987). Limitations of carbon dioxide lasers for treatment of port-wine stains. *Arch Dermatol*, Vol.123, No.1, (January 1987), pp. 71-73, ISSN (Printed): 0340-3696 (Online): 1432-069X
- Gemert, M.J.C. van; Welch, A.J.; Pickering, J.W. & Tan, O.T. (1995). Laser Treatment of Port Wine Stains, In: *Optical-Thermal Response of laser-Irradiated Tissue*, A.J. Welch & M.J.C. van Gemert, (Ed.), 789-829, Plenum Press, ISBN 0-306-44926-9, New York
- Gemert, M.J.C. van; Smithies, D.J.; Verkruyse, W.; Milner, T.E. and Nelson, J.S. (1997). Wavelengths for port wine stain laser treatment: influence of vessel radius and skin anatomy. *Phys Med Biol*, Vol.42, No.1, (January 1997), pp. 41-50, ISSN 0031-9155
- Gilchrest, B.A.; Rosen, S. & Noe, J.M. (1982). Chilling port wine stains improves the response to argon laser therapy. *J Plast Reconstr Surg*, Vol.69, No.2, (February 1982), pp. 278-283, ISSN 0032-1052 (Print), 1529-4242 (Online)
- Hammes, S. & Raulin, C. (2005). Evaluation of different temperatures in cold air cooling with pulsed-dye laser treatment of facial telangiectasia. *Lasers in Surgery and Medicine*, Vol.36, No.2, (February 2005), pp. 136-140, ISSN 0196-8092
- Ishimaru, A. (1989). Diffusion of light in turbid media. *Appl Opt*, Vol.28, No.12, (June 1989), pp. 2210-2215, ISSN 1559-128X (Print) 2155-3165 (Online)
- Jacques, S.L. & Wang, L.H. (1995). Monte Carlo Modeling of Light Transport in Tissues, In: *Optical-Thermal Response of laser-Irradiated Tissue*, A.J. Welch & M.J.C. van Gemert, (Ed.), 73-100, Plenum Press, ISBN 0-306-44926-9, New York
- Jia, W.C.; Aguilar, G.; Wang, G.-X. & Nelson, J.S. (2004). Heat transfer dynamics during cryogen spray cooling of substrate at different initial temperatures. *Phys Med Biol*, Vol. 49, No.23, (December 2004), pp. 5295-5308. ISSN 0031-9155
- Jia, W.; Aguilar, G.; Verkruyse, W.; Franco, W. & Nelson, J.S. (2006). Improvement of port wine stain laser therapy by skin preheating prior to cryogen spray cooling: a numerical simulation. *Lasers in Surgery and Medicine*, Vol.38, No.2, (February 2006), pp. 155-162. ISSN 0196-8092
- Jia, W.C.; Choi, B.; Franco, W.; Lotfi, J.; Majaron, B.; Aguilar, G.; & Nelson, J.S. (2007). Treatment of cutaneous vascular lesions using multiple-intermittent cryogen spurts and two-wavelength laser pulses: numerical and animal studies. *Lasers in Surgery and Medicine*, Vol.39, No.6, (July 2007), pp. 494-503, ISSN 0196-8092
- Keijzer, M.; Pickering, J.W. & van Gemert, M.J.C. (1991). Laser beam diameter for port wine stain treatment. *Lasers in Surgery and Medicine*, Vol.11, No.6, (October 1991), pp. 601-605, ISSN 0196-8092
- Kelly, K.M.; Choi B.; McFarlane, S; *et al.* (2005). Description and analysis of treatments for port-wine stain birthmarks. *Arch Facial Plast Surg*, Vol.7, No.5, (October 2005), pp. 287-94, ISSN 1521-2491
- Kienle, A. & Hibst, R. (1995). A new optimal wavelength for treatment of port wine stains? *Phys Med Biol*, Vol.40, No.10, (October 1995), pp. 1559-76, ISSN 0031-9155
- Kienle, A. & Hibst, R. (1997). Optimal parameters for laser treatment of leg telangiectasia. *Lasers in Surgery and Medicine*, Vol.20, No.3, (December 1998), pp. 346-353, ISSN 0196-8092

- Lahaye C.T.W. & van Gemert, M.J.C. (1985). Optimal laser parameters for port wine stain therapy: a theoretical approach. *Phys Med Biol*, Vol.30, No.6, (June 1985), pp.573-87, ISSN 0031-9155
- Lanigan, S. W. (2000). *Lasers in Dermatology*, Springer, London, ISBN 1852332778
- Li, D.; He, Y.L.; Liu, Y.W. & Wang, G.-X. (2007a), Numerical analysis of cryogen spray cooling of skin in dermatologic laser surgery using realistic boundary conditions. *Proceedings of 22th Int. Congress Refrigeration conference*, (July) 2007, Beijing, China
- Li, D.; He, Y.L.; Wang, G.-X.; Xiao, J. & Liu, Y.W. (2007b), Numerical analysis of cold injury of skin in cryogen spray cooling for dermatologic laser surgery. *Proceedings of 2007 ASME International Mechanical Engineering Congress*, IMECE2007-43876, Nov. 2007, Seattle, Washington, ISBN 0-7918-4302-5
- Li, D.; Wang, G.-X. & He, Y.L. (2011), Criteria for section of voxel size and photon number in Monte Carlo Simulation, to be submitted
- Lucassen, G.W.; Svaasand, L.O.; Verkruysse, W. & van Gemert, M.J.C. (1995). Laser energy threshold for thermal vascular injury in a port wine stain skin model. *Laser Med Sci*, Vol.10, No.4, (December 1995), pp. 231-234, 0268-8921 (Print), 1435-604X (Online)
- Lucassen, G.W.; Verkruysse, W.; Keijzer, M. & van Gerner, M.J.C. (1996). Light distribution in a port wine stain model containing multiple cylindrical and curved blood vessels. *Lasers in Surgery and Medicine*, Vol.18, No.4, (April 1996), pp. 345-357, ISSN 0196-8092
- Majaron, B.; Verkruysse, W.; Kelly, K.M.; & Nelson, J.S. (2001). Er:YAG laser skin resurfacing using repetitive long-pulse exposure and cryogen spray cooling: II. theoretical analysis. *Lasers in Surgery and Medicine*, Vol.28, No.2, (February 2001), pp. 131-137, ISSN 0196-8092
- Miller, I.D. & Veith, A. R. (1993). Optical modelling of light distributions in skin tissue following laser irradiation. *Lasers in Surgery and Medicine*, Vol.13, No.5, (May 1993), pp. 565-571, ISSN 0196-8092
- Nelson, J.S.; Milner, T.E.; Anvari, B.; Tanenbaum, B.S.; Kimel, S.; Svaasand, L.O.; & Jacques, S.L. (1995). Dynamic epidermal cooling during pulsed laser treatment of port-wine stain: A new methodology with preliminary clinical evaluation. *Arch Dermatol*, Vol.131, No.6, (June 1995), pp. 695-700, ISSN 1538-3652 (Print), 0003-987X (Online)
- Niemz, M.H.; (1996). *Laser-Tissue Interactions: Fundamentals and Applications*, Springer Berlin Heidelberg, New York. Hardcover, ISBN 978-3-540-40553-5 Softcover, ISBN 978-3-540-72191-8
- Orten S.S.; Waner M.; Flock S.; Roberson P.K.; Kincannon J. (1996). Port wine stains: an assessment of five years of treatment. *Arch Otolaryngol Head Neck Surg*, Vol.122, No.11, (November 1996), pp. 1174-9. ISSN 0886-4470 (Print) 1538-361X (Online)
- Pearce, J. & Thomsen, S. (1995). Rate Process Analysis of Thermal Damage, In: *Optical-Thermal Response of laser-Irradiated Tissue*, A.J. Welch & M.J.C. van Gemert, (Ed.), 561-606, Plenum Press, ISBN 0-306-44926-9, New York
- Pfefer, T.J.; Barton, J.K.; Chan, E.K.; Ducros, M.G.; Sorg, B.S.; Milner, T.E.; Nelson, J.S. & Welch, A.J. (1996). A three dimensional modular adaptable grid numerical model for light propagation during laser irradiation of skin tissue. *IEEE Journal of Selected in Quantum Electronics*, Vol.4, No.4, (December 1996), pp. 934-942, ISSN 1077-260X

- Pfefer, T.J.; Smithies, D.J.; Milner, T.E.; van Gemert, M.J.C.; Nelson, J.S. & Welch, A.J. (2000). Bioheat transfer analysis of cryogen spray cooling during laser treatment of Port Wine Stains. *Lasers in Surgery and Medicine*, Vol.26, No.2, (February 2000), pp. 145-157, ISSN 0196-8092
- Pickering, J.W.; Butler, P.H.; Ring, B.J. & Walker, E.P. (1989). Computed temperature distributions around ectatic capillaries exposed to yellow (578 nm) laser light. *Phys Med Biol*, Vol.34, pp. 1247-1258, ISSN 0031-9155
- Pickering, J.W. & van Gemert, M.J.C. (1991). 585 nm for the laser treatment of port wine stains: A possible mechanism. *Lasers in Surgery and Medicine*, Vol.11, No.6, (June 1991), pp. 616-618, ISSN 0196-8092
- Pikkula, B.M.; Torres, J. H.; Tunnell, J.W. & Anvari, B. (2001). Cryogen spray cooling: effects of droplet size and spray density on heat removal. *Lasers in Surgery and Medicine*, Vol. 28, No.2, (February 2001), pp. 103-112, ISSN 0196-8092
- Shafirstein, G.; Bäumlner, W.; Lapidoth, M.; Ferguson, S.; North, P.E. & Waner, M. (2004). A New Mathematical Approach to the Diffusion Approximation Theory for Selective Photothermolysis Modeling and Its Implication In Laser Treatment of Port-Wine Stains. *Lasers in Surgery and Medicine*, Vol. 34, No.4, (April 2004), pp. 335-347, ISSN 196-8092
- Shafirstein, G. & Buckmiller, L.M.; Waner, M. & Bäumlner, W. (2007). Mathematical modeling of selective photothermolysis to aid the treatment of vascular malformations and hemangioma with pulsed dye laser. *Lasers Med Sci*, Vol.22, No.2, (June 2007), pp. 111-118, ISSN 0268-8921(Print), 1435-604X (Online)
- Smithies, D.J. & Butler, P.H. (1995). Modelling the distribution of laser light in port-wine stains with the Monte Carlo method. *Phys Med Biol*, Vol.40, No.5, (May 1995), pp. 701-33, ISSN 0031-9155
- Tan, O.T.; Morrison, P. & Kurban, A.K. (1990). 585 nm for the treatment of port-wine stains. *Plast Reconstr Surg Med*, Vol.86, No.6, (December 1990), pp. 1112-1117, ISSN 0032-1052 (Print), 1529-4242 (Online)
- Tunnell, J.W.; Nelson, J.S.; Torres, J.H.; & Anvari, B. (2000). Epidermal protection with cryogen spray cooling during high fluence pulsed dye laser irradiation: an ex vivo study. *Lasers in Surgery and Medicine*, Vol.27, No.4, (April 2000), pp. 373-383, ISSN 0196-8092
- Tunnell, J.W.; Wang, L.V. & Anvari, B. (2003). Optimum pulse duration and radiant exposure for vascular laser therapy of dark portwine skin: A theoretical study. *Appl Opt*, Vol.42, No.7, (July 2003), pp. 1367-1378, ISSN 1559-128X (Print), 2155-3165 (Online)
- Verkruyssen, W.; Pickering, J.W.; Beek, J.F.; Keijzer, M.; van Gemert, M.J.C. (1993). Modeling the effect of wavelength on the pulsed dye laser treatment of port wine stains. *Appl Opt*, Vol.32, No.4, (February 1993), pp. 393-8, ISSN 1559-128X (Print), 2155-3165 (Online)
- Wang, L.H.; Jacques, S.L. & Zheng, L.Q. (1995). MCML-Monte Carlo modeling of light transport in multi-layered tissues. *Comp Meth Prog Biol*, Vol.47, No.2, (July 1995), pp. 131-146, ISSN 0169-2607
- Wilson, B.C. & Adam, G. (1983). A Monte-Carlo model for the absorption and flux distribution of light in tissue. *Med Phys*, Vol.10, No.6, (December 1983), pp. 824-830, ISSN 0094-2405

- Zhou, Z.; Xin, H.; Chen, B. & Wang, G.-X. (2008a). Theoretical Evaporation Model of a Single Droplet in Laser Treatment of PWS in Conjunction with Cryogen Spray Cooling. *Proceedings of 2008 ASME Summer Heat Transfer Conference*, HT2008-56063, Aug. 10-14, 2008, Hyatt Regency Riverfront, Jacksonville, Florida, ISBN: 978-0-7918-4849-4
- Zhou, Z.; Xin, H.; Chen, B. & Wang, G.-X. (2008b). Single Droplet Evaporation Model in Laser Treatment of PWS in Conjunction with Cryogen Spray Cooling. *Proceedings of 2008 International Conference on Bio-Medical Engineering and Informatics*, Vol. 1, pp. 551-556, May 28-30, Sanya, Hainan, China, ISBN: 978-0-7695-3118-2



## **Developments in Heat Transfer**

Edited by Dr. Marco Aurelio Dos Santos Bernardes

ISBN 978-953-307-569-3

Hard cover, 688 pages

**Publisher** InTech

**Published online** 15, September, 2011

**Published in print edition** September, 2011

This book comprises heat transfer fundamental concepts and modes (specifically conduction, convection and radiation), bioheat, entransy theory development, micro heat transfer, high temperature applications, turbulent shear flows, mass transfer, heat pipes, design optimization, medical therapies, fiber-optics, heat transfer in surfactant solutions, landmine detection, heat exchangers, radiant floor, packed bed thermal storage systems, inverse space marching method, heat transfer in short slot ducts, freezing and drying mechanisms, variable property effects in heat transfer, heat transfer in electronics and process industries, fission-track thermochronology, combustion, heat transfer in liquid metal flows, human comfort in underground mining, heat transfer on electrical discharge machining and mixing convection. The experimental and theoretical investigations, assessment and enhancement techniques illustrated here aspire to be useful for many researchers, scientists, engineers and graduate students.

### **How to reference**

In order to correctly reference this scholarly work, feel free to copy and paste the following:

Dong Li, Ya-Ling He and Guo-Xiang Wang (2011). Thermal Modelling for Laser Treatment of Port Wine Stains, *Developments in Heat Transfer*, Dr. Marco Aurelio Dos Santos Bernardes (Ed.), ISBN: 978-953-307-569-3, InTech, Available from: <http://www.intechopen.com/books/developments-in-heat-transfer/thermal-modelling-for-laser-treatment-of-port-wine-stains>

# **INTECH**

open science | open minds

### **InTech Europe**

University Campus STeP Ri  
Slavka Krautzeka 83/A  
51000 Rijeka, Croatia  
Phone: +385 (51) 770 447  
Fax: +385 (51) 686 166  
[www.intechopen.com](http://www.intechopen.com)

### **InTech China**

Unit 405, Office Block, Hotel Equatorial Shanghai  
No.65, Yan An Road (West), Shanghai, 200040, China  
中国上海市延安西路65号上海国际贵都大饭店办公楼405单元  
Phone: +86-21-62489820  
Fax: +86-21-62489821

© 2011 The Author(s). Licensee IntechOpen. This chapter is distributed under the terms of the [Creative Commons Attribution-NonCommercial-ShareAlike-3.0 License](#), which permits use, distribution and reproduction for non-commercial purposes, provided the original is properly cited and derivative works building on this content are distributed under the same license.